Robust fault detection and isolation technique for single-input/single-output closed-loop control systems that exhibit actuator and sensor faults

Izadi-Zamanabadi, Roozbeh; Alavi, S. M. Mahdi; Hayes, M. J.

Published in:
IET Control Theory and Applications

DOI (link to publication from Publisher):
10.1049/iet-cta:20070382

Publication date:
2008

Document Version
Publisher's PDF, also known as Version of record

Published in IET Control Theory and Applications
Received on 15th October 2007
Revised on 10th April 2008
doi: 10.1049/iet-cta:20070382

ISSN 1751-8644

Robust fault detection and isolation technique for single-input/single-output closed-loop control systems that exhibit actuator and sensor faults

S.M. Mahdi Alavi[1] *R. Izadi-Zamanabadi*[2] *M.J. Hayes*[1]

[1]*Department of Electronic and Computer Engineering, University of Limerick, Ireland*
[2]*Section for Automation and Control, Department of Electronic Systems, Aalborg University, Denmark*
E-mail: Mahdi.S.Alavi@ul.ie

Abstract: An integrated quantitative feedback design and frequency-based fault detection and isolation (FDI) approach is presented for single-input/single-output systems. A novel design methodology, based on shaping the system frequency response, is proposed to generate an appropriate residual signal that is sensitive to actuator and sensor faults in the presence of model uncertainty and exogenous unknown (unmeasured) disturbances. The key features of this technique are: (1) the uncertain phase information is fully addressed by the design equations, resulting in a minimally conservative over-design and (2) a graphical environment is provided for the design of fault detection (FD) filter, which is intuitively appealing from an engineering perspective. The FD filter can easily be obtained by manually shaping the frequency response into the complex plane. The question of interaction between actuator and sensor fault residuals is also considered. It is discussed how the actuator and sensor faults are distinguished from each other by appropriately defining FDI threshold values. The efficiency of the proposed method is demonstrated on a single machine infinite bus power system wherein a stabilised coordinate power system incorporating a robust FDI capability is achieved.

1 Introduction

The goal of reliability and fault tolerance in a control system design requires that fault detection and isolation (FDI) (The fault can be isolated if the faulty component is determined, [1]) modules perform well under a variety of internal and external conditions such as unknown disturbances, actuator and sensor faults, plant uncertainty and noise. Model-based FDI has been the subject of significant attention in recent years (see [1–4] and references therein). The main objective of a model-based FDI paradigm is to generate a so-called residual that is sensitive to exogenous fault signals. In this context, the question of joint disturbance decoupling and robustness of the attendant residual signal in the presence of significant plant uncertainty is the specific question that is considered in this paper. A great deal of the published research on this issue concentrates on observer-based and parameter estimation methods [5–8]. However, the authors feel that such methods provide solutions that do not yield an easy interpretation that can manage the trade-off between disturbance decoupling and fault detection (FD) in a closed-loop configuration. Moreover, the necessary on-line algorithms that are required for parameter estimation are time-consuming, and can lead to a significant increase in the complexity of the design.

The focus of this work therefore is the determination of a robust frequency-domain approach wherein some insight is provided regarding the necessary design trade-off between disturbance decoupling and FD. The literature suggests several robust FD techniques in this respect, which are

motivated by some combination of H_∞/H_2, H_∞/μ and H_∞/linear matrix inequality (LMI) paradigms, [9–14]. However, the inherent conservatism within such frequency-domain H_∞-based approaches can lead to high-order designs, without any guarantee of a priori levels of robust performance. The aim in [15] is to minimise the effect of faults on the system performance for a servohydraulic positioning system. In this paper, however, a specific theme of the work is to design appropriate filters that can detect faults as well as addressing certain robustness objectives. Moreover, a generalised structure is proposed that seeks to increase the range of applicability for a quantitative feedback theory (QFT)-based approach to a closed-loop FDI system.

Having determined an appropriate residual, the next step in the FDI technique is the so-called residual evaluation that is necessary in order to be able to make accurate detection and isolation decisions. Because of the inevitable existence of noise and model errors, the residuals are never zero, even if there is no fault and the disturbance is decoupled perfectly. Therefore a detection decision requires that residuals be compared with a so-called threshold value, obtained empirically (generally) or theoretically. Again, a significant literature exists relating to the determination of such an appropriate threshold value [1, 3, 11, 16]. It is noted that most of the aforementioned techniques are presented for open-loop systems and concentrate on FD purposes. Now given that industrial systems, (usually of necessity), work under feedback control, any FDI algorithm should be capable of being applied in such a scenario. In [9, 12], H_∞-based methodologies for such an integrated closed-loop FD system have been presented. However, the fault isolation technique under feedback control is still a major unresolved theme.

In this paper, a novel two-degree-of-freedom robust FDI technique is presented for single-input/single-output (SISO) closed-loop systems. The disturbance decoupling and the subsequent step of robust residual generation are addressed via the following two-stage procedure. In step (1), the effects of exogenous disturbances appearing on the special frequency range as well as the effect of model uncertainty are minimised by using an appropriate feedback compensator. In step (2), an FD filter that tracks the pre-specified residual reference model is synthesised. To have a feasible solution to the proposed min–max problem, the frequency ranges of the simultaneous disturbance attenuation and FD are separated based on the system dynamic, control and FD objectives. The FD problem is formulated so that the effect of the feedback compensator, designed a priori, is fully considered in the second step, thereby minimising over-design. A well known residual evaluation function is then utilised to isolate the faults and make proper alarms. This paper is an extension of [17] to the system with both actuator and sensor faults.

The particular contribution of this work can be summarised as:

- The graphical design environment of the FD filter, proposed in this paper, is intuitively appealing from an engineering perspective. The FD filter can easily be obtained through a manual shaping of the frequency response in the complex plane. The resulting FD filter will be much simpler than the existing H_∞/H_2, H_∞/μ and H_∞/LMI paradigms.

- For a system having both actuator and sensor faults, there is an unavoidable interaction between actuator and sensor fault residuals and evaluation signals. Particular reference to this cross-coupling effect is presented here. The benchmark power system example that is considered provides an easily reproducible concrete example that will be of significant practical benefit to researchers in the area. Furthermore, the selection of FDI threshold values that can appropriately distinguish between actuator and sensor faults is a specific challenge in this regard, which receives special attention. In particular, it is explained how the FDI threshold values can be adjusted in an intuitive fashion so as to accurately distinguish an actuator fault from a sensor fault.

- A feature of this procedure is that the uncertain phase information is fully addressed by the design equations, resulting in a minimally conservative design. In this sense, the proposed approach should be viewed as optimal for non-minimum phase and time-delay systems.

- An extension to the case of multiple input(output) disturbances and multiple actuator(sensor) faults is also discussed.

This paper is organised as follows. In Section 3, the FDI scheme and the objectives of the paper are outlined. In Section 4, the feedback compensator is designed to attenuate the effects of disturbances and model uncertainty. The design of the detection filters is then presented in Section 5. Section 6 deals with a method of residual evaluation and fault isolation. Finally, the efficiency of the proposed methodology is demonstrated using a single machine infinite bus (SMIB) power system in Section 7. In addition, a comparative study of FDI methods based on H_∞/H_2 and H_∞/LMI paradigms are carried out in this section.

2 Notation

The general notations throughout the paper are as follows. Vector and matrix are shown by 'bold' letters. $\mathbf{x} \in \mathbb{R}^n$ is system state vector and $u \in \mathbb{R}$ is a control signal. ($\mathbf{A}$, $\mathbf{B}$, $\mathbf{C}$, $\mathbf{D}$) are the system matrices for the open-loop system. ($\mathbf{B}_f$, $\mathbf{D}_f$, $\mathbf{B}_d$, $\mathbf{D}_d$) are fault and disturbance distribution matrices. $\mathbf{A}^T$ denotes transpose of matrix $\mathbf{A}$. If $\mathbf{A}$ is a symmetric matrix, $\mathbf{A} > (\geq) 0$ denotes the positive (positive semi-definite) matrix. Likewise, If $\mathbf{A}$ is a symmetric matrix,

IET Control Theory Appl., 2008, Vol. 2, No. 11, pp. 951–965
doi: 10.1049/iet-cta:20070382

$\mathbf{A} < (\leq) 0$ denotes the negative (negative semi-definite) matrix. The space of rational, stable and proper transfer functions is denoted by $\mathcal{RH}_\infty$.

3 System description

Fig. 1 presents a block diagram of the design methodology considered in this work. $P(s)$ represents a SISO linear(ised) plant transfer function (TF) within the uncertainty region $\{\mathcal{P}\}$. $d_1(t) \in \mathbb{R}$ and $d_2(t) \in \mathbb{R}$ denote unknown exogenous input and output disturbances that may be, respectively, added to the control signal and measurement output. Likewise, $f_1(t) \in \mathbb{R}$ and $f_2(t) \in \mathbb{R}$ represent actuator and sensor faults that may be, respectively, added to the control signal and measurement output. $y_m(t) \in \mathbb{R}$ represents the output measurement that is to be compared with reference (or command) signal $c(t) \in \mathbb{R}$.

The objective is to generate an appropriate actuator-fault residual $r_1(t)$ and sensor-fault residual $r_2(t)$, which are sensitive, respectively, to $f_1(t)$ and $f_2(t)$, and are robust against disturbances and plant uncertainties, [11, 13].

To achieve both control (robust stability and performance) and FD objectives, the proposed technique in this paper is a two-degree-of-freedom technique consisting of:

1. A feedback controller design stage, $G(s)$ in $\mathcal{RH}_\infty$, which achieves a satisfactory level of robustness and disturbance attenuation.

2. An FD filter design stage for $Q_i(s)$, $i = 1, 2$ in $\mathcal{RH}_\infty$ that minimises the difference between the actual and reference residual models.

3. A residual evaluation stage that generates appropriate fault alarms and provides acceptable levels of avoidance of false alarms.

An extension to the multiple input (output) disturbances and multiple actuator (sensor) faults is also discussed.

4 Design of feedback compensator $G(s)$

At the first step, feedback compensator $G(s)$ is primarily designed to achieve a satisfactory level of robust stability and robust performance in spite of model uncertainty and disturbance when the system is fault free. Clearly, robustness can be achieved using a variety of controller design paradigms. For instance, the H_∞ theory [18] or QFT [19] can be used in this stage. The QFT loop-shaping paradigm introduced by Horowitz and Sidi in [20] is essentially a frequency-domain technique using standard feedback architecture to achieve client-specified levels of desired performance over a region of uncertainty determined a priori by the engineer. The methodology requires that some desired constraints be generated in terms of the closed-loop frequency response, which in turn lead to design bounds in the loop function on the Nichols chart. $G(s)$ is designed by shaping the loop gain function such that the design bounds are satisfied. There are a number of reasons why it can be expected that a quantitative feedback approach can offer significant benefits when designing a coordinate closed-loop system that exhibits satisfactory FDI capabilities. These include: (i) the ability of a QFT approach to handle a wide range of parametric uncertainty with minimal attendant conservatism (see [19–21] for details), (ii) the presentation of design requirements as graphical constraints for a set of frequencies of interest is intuitively appealing from an engineering perspective and (iii) the use of the logarithmic complex plane for the design of the feedback compensator, utilising the Nichols chart, provides useful insight into system design trade-offs.

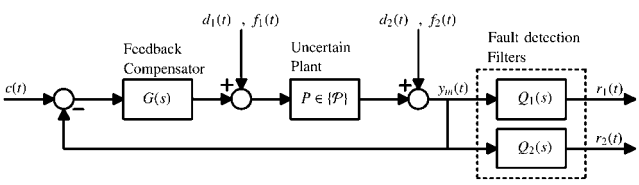

Figure 1 *Two-degree-of-freedom simultaneous control and FDI structure*

The design of $G(s)$ is governed by the following assumptions:

Assumptions 1

a. Theoretically, there is no analytical solution to simultaneously minimise input (output) disturbances and maximise actuator (sensor) faults for FD purposes at the same frequency. This issue is relaxed as follows. It is assumed that the input (output) disturbance attenuation over the frequency range of Λ_1 (Λ_2) is desirable. Also, it is assumed that Ω_1 (Ω_2) represents the frequency range where the actuator (sensor) FD is likely to be concentrated, and $\Lambda_i \neq \Omega_i$ for $i = 1, 2$.

b. It is assumed that $d_i(t)$, $i = 1, 2$ are bounded.

Bearing the above constraints in mind, $G(s)$ is designed via the following two stage procedure.

4.1 Design constraints

In order to design an appropriate feedback controller, the following set of desired specifications are introduced.

1. *Disturbance rejection constraint*: To minimize the effect of input and output disturbances, (1) and (2) are, respectively, employed to over bound the TF from $d_1(t)$ and $d_2(t)$ to $y_m(t)$ with appropriate disturbance rejection weighting

doi: 10.1049/iet-cta:20070382

functions $W_{d_1}(s)$ and $W_{d_2}(s)$

$$|N_1(s)|_{s=j\omega} \triangleq \left|\frac{P(s)}{1+G(s)P(s)}\right|_{s=j\omega} \leq \left|W_{d_1}(j\omega)\right|$$
$$\forall P \in \{\mathcal{P}\} \quad \text{and} \quad \omega \in \Lambda_1 \tag{1}$$

and

$$|N_2(s)|_{s=j\omega} \triangleq \left|\frac{1}{1+G(s)P(s)}\right|_{s=j\omega} \leq \left|W_{d_2}(j\omega)\right|$$
$$\forall P \in \{\mathcal{P}\} \quad \text{and} \quad \omega \in \Lambda_2 \tag{2}$$

where Λ_i, $i = 1, 2$ represent the frequency ranges that are defined a priori by the engineer as to where the attenuation of disturbances are likely to be of most significance.

It is noted that for the case of multiple input(output) disturbances, the TF from each disturbance to $y_m(t)$ is over bounded with an appropriate disturbance rejection weighting function.

2. *Tracking constraint*: It is standard practice in QFT design to locate the closed-loop TF response between the lower and upper bounds $T_L(s)$ and $T_U(s)$, according to

$$|T_L(j\omega)| \leq \left|\frac{G(s)P(s)}{1+G(s)P(s)}\right|_{s=j\omega} \leq |T_U(j\omega)|$$
$$\forall P \in \{\mathcal{P}\} \quad \text{and} \quad \omega \in [0, \omega_b] \tag{3}$$

$T_L(s)$ and $T_U(s)$ are again typically defined a priori by the engineer based on a performance requirement analysis for the system at hand using conventional time-domain concepts such as settling time and\or overshoot. It should be noted that experience has shown that the optimum selection of ω_b is dependent on the nature of the system and the desired specifications, [19, 21].

3. *Robust stability constraint*: To achieve robust stability within $[0, \omega_b]$, it is sufficient to design the feedback compensator such that the loop function, $l(s) = P_0(s)G(s)$ does not intersect the critical point $(-180, 0\ \text{dB})$. $P_0(s)$ denotes the nominal plant. However, the following constraint on the complementary sensitivity TF should also be considered at higher frequencies, thereby incorporating the notion of gain and phase margins into the problem specification

$$\left|\frac{G(s)P(s)}{1+G(s)P(s)}\right|_{s=j\omega} \leq \mu$$
$$\forall P \in \{\mathcal{P}\} \quad \text{and} \quad \omega \geq \omega_b \tag{4}$$

This criterion corresponds to the lower bounds of the gain margin of $K_M = 1 + 1/\mu$ and the phase margin angle of $\phi_M = 180^\circ - \cos^{-1}(0.5/\mu^2 - 1)$, [22]. Experience has shown that a selection of a range of frequencies up to a maximum of $10\omega_b$ has been found to be sufficient to ensure that performance is acceptable over the bandwidth of the design. However it should again be noted that the precise selection of the set of frequencies greater than ω_b to be considered in this instance is also a matter on which engineering judgement and experience tend to have an impact.

4.2 Loop-shaping procedure

At each design frequency, the solution of (1), (2), (3) and (4) will result in QFT design bounds which divide Nichols chart into acceptable and unacceptable regions. The intersection of the bounds at each design frequency is the value that is taken for the design of the feedback compensator. $G(s)$ is designed by adding appropriate poles and zeros to the nominal loop function $l(s)$ such that $l(s)$ satisfies the worst-case design constraint for the bounds at each frequency. For robustness, the nominal loop function must be shaped such that the frequency response lies above the design bounds at each frequency of interest and does not enter the U-contours. The appearance of U-contours at high frequencies arises from the fact that as $\omega \to \infty$, the limiting value of the plant TF approaches $\lim_{\omega\to\infty} P(j\omega) = \tilde{K}/s^{\rho}$, where $\tilde{K}$ is a real value and ρ represents the excess of poles over zeros of $P(s)$. Finally, the critical point $(-180^\circ, 0\ \text{dB})$ must also be avoided, [19, 21].

5 Design of FD filter $Q_i(s)$, $i = 1,2$

Having designed an appropriate $G(s)$, step 2 of a mixed control and FDI system is the synthesis of an FD filter $Q_i(s)$ that generates the corresponding robust residual $r_i(t)$, for $i = 1, 2$. The basis for the work relies on the assumption that it is feasible to construct a reference (i.e. desired) model for the residual in both actuator and sensor fault cases based on the proposed methodology in [11, 23]. The actuator and sensor faults residuals are denoted by M_1 and M_2 respectively. The objective is then to obtain $Q_i(s)$ such that the TF from $f_i(t)$ to the actual residual, $r_i(t)$, becomes matched to the pre-defined residual reference model $M_i(s)$ through the satisfaction of the following constraint

$$|M_i(j\omega) - Q_i(j\omega)N_i(j\omega)| \leq \left|E_{d_i}(j\omega)\right|$$
$$\forall P \in \{\mathcal{P}\} \quad \text{and} \quad \omega \in \Omega_i \neq \Lambda_i, \quad \text{for } i = 1, 2 \tag{5}$$

For the actuator FD, $i = 1$ and $N_1(j\omega) = P(j\omega)/(1 + P(j\omega)G(j\omega))$. For the sensor FD, $i = 2$ and $N_2(j\omega) = 1/(1 + P(j\omega)G(j\omega))$. $E_{d_i}(s)$, $i = 1, 2$ represent the desired dynamic behaviour of the error between the residual reference models and corresponding actual models. Ω_i represents the frequency region where the energy of the fault is likely to be concentrated.

Remark 1

a. It is clear that there is no conflict between the input disturbance attenuation and the actuator FD, because of

IET Control Theory Appl., 2008, Vol. 2, No. 11, pp. 951–965
doi: 10.1049/iet-cta:20070382

the relaxation that has been considered for the frequency ranges of control and FD objectives. The same result is valid for the output disturbance attenuation and the sensor FD. It should be noted that the frequency response of $G(s)$ over the frequency that is not incorporated within the feedback compensator design stage may adversely affect the purposes of the FD. However, it is clear that (5) fully captures the effects of $G(s)$ over the frequency range that FD is likely to be required. Moreover, by writing the TFs from the fault signals to the system output, it can be shown in a straightforward manner that the feedback compensator considered here cannot eliminate the aforementioned faults.

b. It is emphasised that since in most cases the higher-frequency response of the plant is nearby zero (because the plants are mostly strictly proper), the detection of the actuator fault (appearing at a higher frequency, which is the case in this paper) is a rather difficult FD problem that is worthy of attention.

c. By defining $S(s) = 1/(1 + P(s)G(s))$ as a sensitivity function of the closed-loop system, it follows from (1) and (2) that: 'the smaller the sensitivity TF, the better the robustness to exogenous disturbances'. However, it also follows from (5) that a large reduction of the sensitivity function results in an extra cost being placed on $Q_i(s)$ to achieve the desired errors $E_{d_i}(s)$. Coupling this fact with Assumption 1a), it is clear that simultaneous input (output) disturbance attenuation and actuator (sensor) FD at the same frequency range can be managed by making a suitable trade-off between the robustness weighing functions and $E_{d_i}(s)$.

5.1 Residual reference models:

The method proposed in [11, 24] is adopted here to obtain the residual reference models $M_i(s)$, for $i = 1, 2$. Consider the uncertain system given by

$$\begin{aligned} \dot{\mathbf{x}} &= (\mathbf{A}_0 + \Delta\mathbf{A})\mathbf{x} + (\mathbf{B}_0 + \Delta\mathbf{B})u + \mathbf{B}_{\mathrm{f}} f_1 + \mathbf{B}_{\mathrm{d}} d_1 \\ y_m &= \mathbf{C}\mathbf{x} + \mathbf{D}u + \mathbf{D}_{\mathrm{f}} f_2 + \mathbf{D}_{\mathrm{d}} d_2 \end{aligned} \tag{6}$$

where $\mathbf{A}_0$ and $\mathbf{B}_0$ are the nominal plant matrices. $\Delta\mathbf{A}$ and $\Delta\mathbf{B}$ represent modelling errors (plant uncertainty) in the form of

$$[\Delta\mathbf{A} \quad \Delta\mathbf{B}] = [\mathbf{E}_1\mathbf{\Sigma}_1\mathbf{F}_1 \quad \mathbf{E}_2\mathbf{\Sigma}_2\mathbf{F}_2] \tag{7}$$

$\mathbf{E}_i$, $\mathbf{F}_i$, $i = 1, 2$ are known matrices and $\mathbf{\Sigma}_i$, $i = 1, 2$ are stochastic matrices such that $\mathbf{\Sigma}_i\mathbf{\Sigma}_i^{\mathrm{T}} \leq \mathbf{I}$.

The generation of the residual reference model relies on the following assumptions, [11]

Assumptions 2

a. $\mathbf{A}_0$ is asymptotically stable.

b. $(\mathbf{C}, \mathbf{A}_0)$ is detectable.

c. $\begin{bmatrix} \mathbf{A}_0 - j\omega\mathbf{I} & \mathbf{B}_{\mathrm{d}} \\ \mathbf{C} & \mathbf{D}_{\mathrm{d}} \end{bmatrix}$ has full row rank for all ω.

Theorem 1: Suppose that Assumptions 2 are satisfied, for (6). Then, the corresponding residual reference model can be obtained by using the following state-space model

$$\begin{aligned} \dot{\mathbf{x}}_f &= (\mathbf{A}_0 - \mathbf{H}^*\mathbf{C})\mathbf{x}_f + \mathbf{B}_{\mathrm{f}} f_1 - \mathbf{H}^*\mathbf{D}_{\mathrm{f}} f_2 + \mathbf{B}_{\mathrm{d}} d_1 - \mathbf{H}^*\mathbf{D}_{\mathrm{d}} d_2 \\ \mathbf{r}_f &= \mathbf{V}^*\mathbf{C}\mathbf{x}_f + \mathbf{V}^*\mathbf{D}_{\mathrm{f}} f_2 + \mathbf{V}^*\mathbf{D}_{\mathrm{d}} d_2 \end{aligned} \tag{8}$$

where

$$\mathbf{H}^* = (\mathbf{B}_{\mathrm{d}}\mathbf{D}_{\mathrm{d}}^{\mathrm{T}} + \mathbf{Y}\mathbf{C}^{\mathrm{T}})\mathbf{X}^{-1} \tag{9}$$

$$\mathbf{V}^* = \mathbf{X}^{-1/2} \tag{10}$$

and $\mathbf{X} = \mathbf{D}_{\mathrm{d}}\mathbf{D}_{\mathrm{d}}^{\mathrm{T}}$ and $\mathbf{Y} \geq \mathbf{0}$ is a solution of the algebraic Riccati equation

$$\bar{\mathbf{A}}^{\mathrm{T}}\mathbf{Y} + \mathbf{Y}\bar{\mathbf{A}} - \mathbf{Y}\bar{\mathbf{B}}\mathbf{X}^{-1}\bar{\mathbf{B}}^{\mathrm{T}}\mathbf{Y} + \bar{\mathbf{Q}} = \mathbf{0} \tag{11}$$

where

$$\begin{aligned} \bar{\mathbf{A}} &= (\mathbf{A}_0 - \mathbf{B}_{\mathrm{d}}\mathbf{D}_{\mathrm{d}}^{\mathrm{T}}\mathbf{X}^{-1}\mathbf{C})^{\mathrm{T}} \\ \bar{\mathbf{B}} &= \mathbf{C}^{\mathrm{T}} \\ \bar{\mathbf{Q}} &= \mathbf{B}_{\mathrm{d}}(\mathbf{I} - \mathbf{D}_{\mathrm{d}}^{\mathrm{T}}\mathbf{X}^{-1}\mathbf{D}_{\mathrm{d}})^2\mathbf{B}_{\mathrm{d}}^{\mathrm{T}} \end{aligned}$$

Proof: See [11, 24].

5.2 Design bounds for shaping $Q_i(s)$, $i = 1, 2$

To obtain the design bounds for shaping $Q_i(s)$, log-polar coordinates are used to transform (5) into a set of quadratic inequalities with known coefficients over the uncertainty region.

Theorem 2: Consider the closed-loop system as shown in Fig. 1. Assume that $G(s)$ has a priori been designed to reduce the effects of disturbance and plant uncertainty according to the proposed methodology in Section 4. Moreover, the residual reference model $M_i(s)$ is obtained through Theorem 1. Then, in order to achieve a pre-defined level of FD given by (5) over the frequency range of Ω_i, it is sufficient to find a $Q_i(s)$ which satisfies the following quadratic inequality for a finite set of $\tilde{\omega} = \{\omega_1, \omega_2, \ldots, \omega_J\}$ over the frequency range Ω_i

$$\rho_2 q_i^2 + \rho_1 q_i + \rho_0 \geq 0 \tag{12}$$

doi: 10.1049/iet-cta:20070382

where

$$\rho_2 = -n_i^2$$
$$\rho_1 = 2n_i m_i \cos(\phi_{n_i} + \phi_{q_i} - \phi_{m_i})$$
$$\rho_0 = -m_i^2 + e_{d_i}^2$$

For actuator FD $i = 1$, and for sensor FD $i = 2$. m_i, n_i, e_{d_i}, q_i, ϕ_{m_i}, ϕ_{n_i}, $\phi_{e_{d_i}}$ and ϕ_{q_i} are provided according to

$$m_i e^{j\phi_{m_i}} = M_i(j\omega_\iota),\ n_i e^{j\phi_{n_i}} = N_i(j\omega_\iota)$$
$$e_{d_i} e^{j\phi_{e_{d_i}}} = E_{d_i}(j\omega_\iota),\ q_i e^{j\phi_{q_i}} = Q_i(\omega_\iota) \tag{13}$$

where ω_ι is a frequency from the finite set of $\tilde{\omega}$.

Proof: Assume that a finite set of frequencies $\tilde{\omega} = \{\omega_1, \omega_2, \ldots, \omega_J\}$ is selected over the frequency range Ω_i. By substituting (13) into (5), it is simple to show that (5) is transformed into the following inequality for each design frequency $\omega_\iota \in \tilde{\omega}$

$$(m_i \cos(\phi_{m_i}) - n_i q_i \cos(\phi_{n_i} + \phi_{q_i}))^2 + (m_i \sin(\phi_{m_i}) - n_i q_i \sin(\phi_{n_i} + \phi_{q_i}))^2 \le e_{d_i}^2 \tag{14}$$

where $M_i(j\omega_\iota)$, $N_i(j\omega_\iota)$ and $E_{d_i}(j\omega_\iota)$ are known and $Q_i(j\omega_\iota)$ is the unknown entity to be tuned. A straightforward calculation of the coefficients of q_i in (14) confirms that it can be directly expressed in the form of (12). □

Equation (12) should be computed and solved for all selected plants over the uncertainty region and for all $\omega_\iota \in \tilde{\omega}$. The solution of (12) for q_i for a given plant case and design frequency, and over $\phi_{q_i} \in [-360, 0]$ will divide the complex plane of $Q_i(s)$ into acceptable and unacceptable regions. The intersection of the regions provides an exact bound for the design of a filter. $Q_i(s)$ should be designed to lie within the provided bounds at each frequency [25, 26].

Remark 2

1. An important question is a how to select $\tilde{\omega}$ from the possible range Ω_i. It is clear that the accuracy of the proposed model-matching problem (5) will improve by using a large set of design frequencies $\tilde{\omega}$. However, it is noted that the design complexity and conservatism are proportional to the number of design frequencies. A large number of design frequencies will increase the number of design bounds to be satisfied, thereby leading to computational burden and a high-order FD filter. Typically, the frequency array $\tilde{\omega}$ is selected intuitively based on the required levels of system performance, the associated computational burden and engineering judgment.

2. This procedure explicitly captures phase information and can, hence, be applied to both minimum and non-minimum phase plants as well as time-delay systems, [25, 27].

3. It should be noted that one possibility for $Q_i(s)$ is that the FD filter be selected as

$$Q_i(s) = M_i(s) N_{i0}^{-1}(s) \tag{15}$$

where $N_{i0}(s)$ is the nominal TF of $N_i(s)$. However, the trivial solution (15) may fail to provide an acceptable performance over the desired uncertainty region. For the non-minimum phase and time-delay plants, (15) results in an unstable FD filter. In such a case, the residual reference model must replicate any right-hand plan (RHP) transmission zeros. This may pose significant challenges, especially if uncertainty exists at the RHP zero locations.

4. The FD filter design can easily be extended to the case of multiple input (output) faults as follows. The residual reference model and corresponding FD bounds are generated for each fault through Theorems 1 and 2. The intersection of the actuator-fault (sensor-fault) bounds at each frequency is the final value that should be considered for shaping $Q_1(s)$ ($Q_2(s)$).

6 Residual evaluation

Suppose that the feedback controller $G(s)$ and the FD filters $Q_i(s)$, $i = 1, 2$ have been designed to meet or exceed the design constraints. To generate an appropriate fault alarm, the following evaluation function can be subsequently introduced on the residual

$$\|r_i\|_2 = \left[\int_{t_1}^{t_2} r_i^2(t)\mathrm{d}t\right]^{1/2} \tag{16}$$

where

$$r_i(t) = r_c(t) + r_{d_i}(t) + r_{f_i}(t), \quad \text{for } i = 1, 2$$

$r_c(t)$, $r_{d_i}(t)$ and $r_{f_i}(t)$ are, respectively, defined as follows

$$r_c(t) = r_i(t)|_{d_i=0, f_i=0}$$
$$r_{d_i}(t) = r_i(t)|_{c=0, f_i=0}$$
$$r_{f_i}(t) = r_i(t)|_{c=0,\ d_i=0} \tag{17}$$

By carrying out the first step of the design procedure a controller $G(s)$ is developed that guarantees a satisfactory level of tracking performance. Consequently, we can assume that $r_c(t) - c(t) \simeq 0$. Therefore the bias of $r_c(t)$ can be ignored using a feed forward of $c(t)$ on the residual signal $r_i(t)$ as shown in Fig. 2. The resulting $\tilde{r}_i(t)$ is then employed for the residual evaluation according to Fig. 2.

$$\tilde{r}_i(t) = r_{d_i}(t) + r_{f_i}(t), \quad \text{for } i = 1, 2$$

doi: 10.1049/iet-cta:20070382

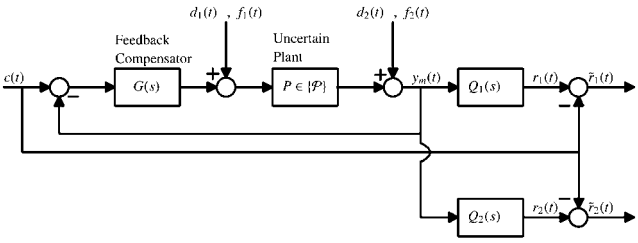

Figure 2 *Modified simultaneous control and FDI structure to eliminate the bias effect of reference signal c(t)*

To generate an appropriate fault alarm, a threshold value J_{th}, is now selected. $\|\tilde{r}_i\|_2$ should be less than J_{th} in the absence of any faults and a failure is declared if $\|\tilde{r}_i\|_2$ exceeds J_{th}. To reduce or prevent false alarms in the presence of unknown disturbances and model uncertainty, a common standard control practice is to select J_{th} as the upper bound of the residual signal in the absence of any fault signal, given by

$$J_{\text{th}} = \sup_{P \in \{\mathcal{P}\}} \|r_{d_i}(t)\|_2 \tag{18}$$

Remark 3: Since a continuous evaluation of the residual signal is impractical, [16], and it is desired that the faults will be detected as early as possible, a detection window, $\tau = t_2 - t_1$, must be determined on the selection of an appropriate J_{th}. Note that, τ must be large enough to distinguish between noise and a sensor failure in the observed signal $\|\tilde{r}_i\|_2$. For more information regarding the selection of such a detection window, the interested reader is directed to consult [16].

7 Illustrative example

An SMIB power system is now considered as a representative example. It should be noted that the nature of such a practical example places an added premium on the synthesis of low-order detection filters, $Q_1(s)$ and $Q_2(s)$, because of the significant practical implementation costs. Fig. 3 shows the functional diagram of the system equipped with a conventional excitation control system. The excitation voltage, E_{fd}, is supplied from the exciter and is controlled by the automatic voltage regulator (AVR) to keep the terminal voltage equal to the reference voltage. Although the AVR is very effective during steady-state operation, it may have a negative influence on the damping of the low-frequency electromechanical oscillations. For this reason, a supplementary control loop, known as the power system stabiliser (PSS), is often added as shown in Fig. 3, in order to achieve an overall improvement in the damping of these electromechanical modes [28].

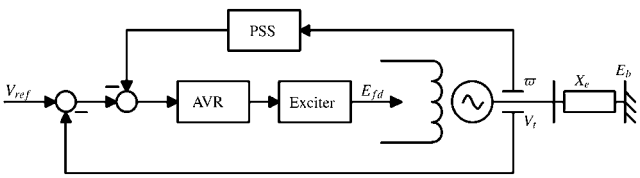

Figure 3 *Schematic diagram of the SMIB power system with AVR and PSS*

By linearising the system about a selected steady-state operating condition, the generator and excitation control system can be modelled as a fourth-order system as shown in Fig. 4. The system dynamic is given as the state-space dynamic model (6) by

$$\mathbf{x} = \begin{pmatrix} \Delta\delta \\ \Delta\varpi \\ \Delta e'_q \\ \Delta E_{\text{f}d} \end{pmatrix}; \quad u = \Delta V_{\text{ref}}; \quad y = \Delta\varpi$$

$$\mathbf{A} = \begin{pmatrix} 0 & \omega_B & 0 & 0 \\ -\dfrac{K_1}{2H} & 0 & -\dfrac{K_2}{2H} & 0 \\ -\dfrac{K_4}{T'_{do}} & 0 & -\dfrac{1}{T'_{do}K_3} & \dfrac{1}{T'_{do}} \\ -\dfrac{K_{\text{A}}K_5}{T_{\text{A}}} & 0 & -\dfrac{K_6K_{\text{A}}}{T_{\text{A}}} & -\dfrac{1}{T_{\text{A}}} \end{pmatrix}; \quad \mathbf{B} = \begin{pmatrix} 0 \\ 0 \\ 0 \\ \dfrac{K_{\text{A}}}{T_{\text{A}}} \end{pmatrix}$$

$$\mathbf{C} = \begin{pmatrix} 0 & 1 & 0 & 0 \end{pmatrix}; \quad \mathbf{D} = 0 \tag{19}$$

The notation used for system variables is given in Appendix 11. The system matrix $\mathbf{A}$ contains uncertain variables K_i, for $i \in \{1, \ldots, 6\}$ where these values are determined by the selected operating condition (equilibrium point) at the linearisation stage. The related equations to compute K_i, for $i \in \{1, \cdots, 6\}$ are provided in Appendix 11. The operating condition is defined by the value of active power, P_m, reactive power, Q_m and the impedance of the transmission line, X_e. To incorporate model uncertainty, it is assumed that these parameters vary independently over the range P_m: 0.4 to 1.0(pu), Q_m: −0.2 to 0.5(pu), and X_e: 0.0 to 0.7(pu), [29]. A random model in the specified range is

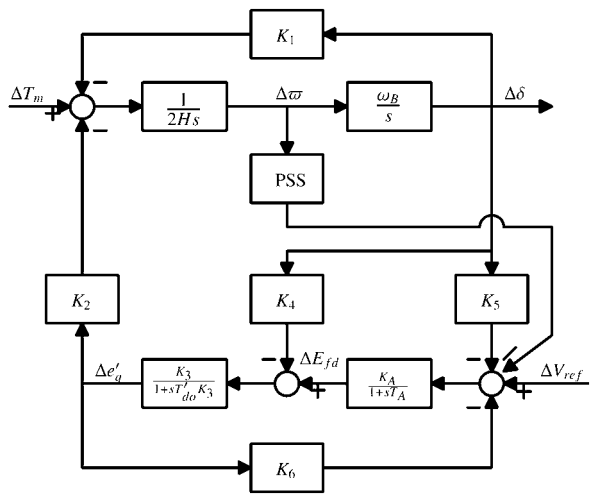

Figure 4 *Block diagram of the linearised SMIB system PSS*

arbitrarily selected as the nominal plant. The system data used for this example is given in Appendix 12.

By adding fault vectors and corresponding detection filters, Fig. 4 can be represented by the unity feedback system as shown in Fig. 5 which is in the appropriate canonical form for the QFT loop-shaping and FD process. Here, the effect of changes in the terminal voltage is treated as an input disturbance to the system.

The TF of generator + AVR is now in the form

$$\text{Generator} + \text{AVR} = \frac{-K_2K_3K_A s}{a_4s^4 + a_3s^3 + a_2s^2 + a_1s + a_0} \quad (20)$$

where

$$\begin{aligned} a_4 &= 2HK_3T'_{do}T_A \\ a_3 &= 2HK_3T'_{do} + 2HT_A \\ a_2 &= 2H + 2HK_3K_6K_A + K_1K_3T'_{do}T_A\omega_B \\ a_1 &= K_1K_3T'_{do}\omega_B + K_1T_A\omega_B - K_2K_3K_4T_A\omega_B \\ a_0 &= K_1\omega_B + K_1K_3K_6K_A\omega_B \\ &\quad - K_2K_3K_4\omega_B - K_2K_3K_5K_A\omega_B \end{aligned}$$

The combined control and diagnosis objectives are defined as follows

A. Design an appropriate feedback controller $G(s)$ to minimise the negative effects of the changes on the terminal voltage for a large range of operating conditions.

B. Design the actuator and sensor FD filters $Q_1(s)$ and $Q_2(s)$ to generate robust fault sensitive residuals $r_1(t)$ and $r_2(t)$.

C. Tune threshold values to detect faults, and make proper alarms.

7.1 Feedback controller design

7.1.1 Design constraints: 1. *Disturbance rejection constraint*: The disturbance rejection ratio is selected as $W_{d_1} = 0.1$ so as to attenuate the effects of the changes in the terminal voltage to less than -10 dB.

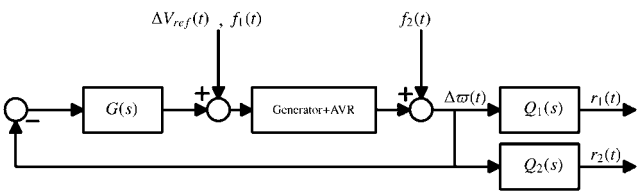

Figure 5 *Block diagram of PSS design using QFT loop shaping problem*

The magnitude plots of the system frequency response inform the generation of an appropriate criterion for the selection of a frequency range for this design cycle. The oscillatory behaviour of the power system, as a result of the poorly damped dominant plant poles, is characterised by peaks in the plant frequency response. Clearly, design frequencies should be located close to these peaks. Fig. 6 shows the plant frequency response for a number of operating points over the uncertainty region. According to Fig. 6, the most dense area for peaks in the magnitude plots of the frequency responses occur within the range $\omega \in [6,\ 12]$ (rad/s). An appropriate range of frequencies for the disturbance attenuation bounds are selected to be $\omega = \{2.5, 6, 7, 8, 9, 10, 12.5\}$ (rad/s).

2. *Robust stability constraint*: For robust stability, choose $\mu = 1.2$ which corresponds to a lower-gain margin of $K_M = 1.833 = 5.26$ (dB) and a phase margin angle of $\phi_M = 49.25°$. Because of maximum peak of system response over the range of $\omega \in [6,\ 12]$(rad/s), the constraint given by (4) is computed for $\omega = \{2.5, 6, 7, 8, 9, 10, 12.5\}$(rad/s).

7.1.2 Loop-shaping design procedure: By using Matlab QFT-Toolbox [30], the design constraints are mapped into so-called QFT design bounds in the Nichols chart at each design frequency. Fig. 7*a* shows the intersection of the bounds that are considered for the tuning process. The loop function $l(s)$, is shaped using an appropriate stabilisation criterion to meet the resulting design bounds. From a practical perspective, a washout time constant of 10 s (i.e. 10 s/(1 + 10 s)) is added to this structure so as to quickly remove low-frequency components (below 0.1 Hz) from the PSS output. The controller structure is also selected as a lead compensator which is popular within the power transmission community because of its ease of implementation. Thus, the final

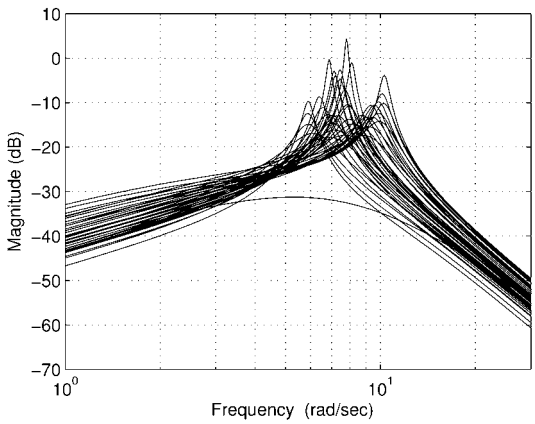

Figure 6 *Magnitude system frequency response for several plants in the uncertainty region*

The figure shows the necessity for using PSS within the range $\omega \in [6, 12]$(rad/s)

IET Control Theory Appl., 2008, Vol. 2, No. 11, pp. 951–965
doi: 10.1049/iet-cta:20070382

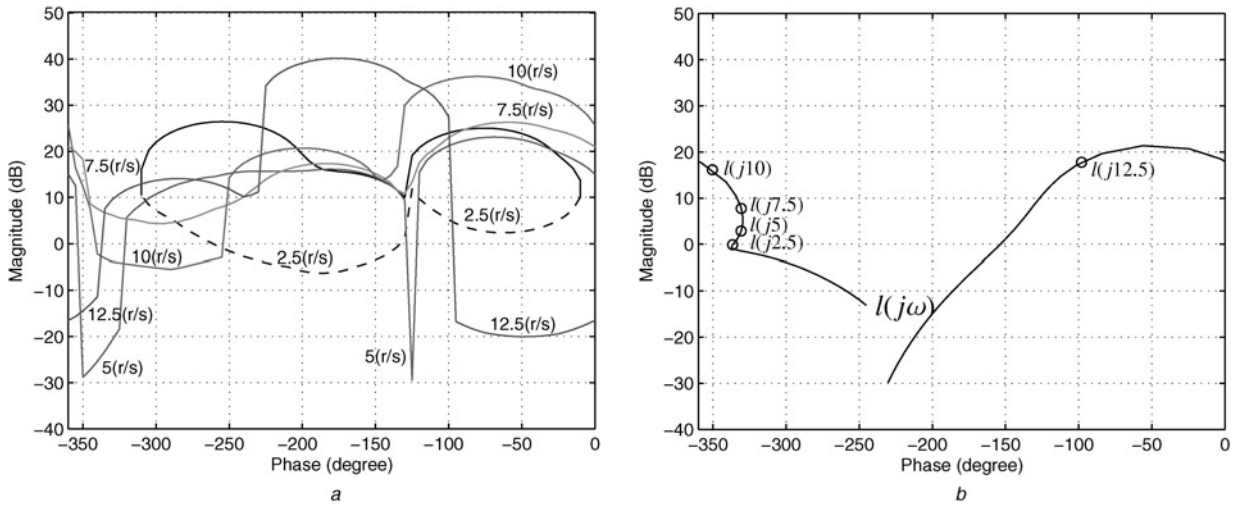

Figure 7 *Illustration of QFT bounds and designed controller in Nichols chart for $\omega = \{2.5, 5, 7.5, 10, 12.5\}$(rad/s)*

For robustness, $l(s)$ must be shaped such that the frequency response lies above the 'solid' line and below the 'dashed' line at each design frequency

The critical point (-180°, 0 dB) must also be avoided (r/s) $\triangleq$ (rad/s)

a QFT design bounds

b Loop-function, $l(s)$

stabiliser, used in the loop-shaping machinery, is taken to be

$$G(s) = K\frac{10s}{1+10s}\frac{(1+T_1 s)^2}{(1+T_2 s)^2} \tag{21}$$

The gain K and the time constants T_1 and T_2 are tuneable parameters. By manually shaping the system frequency response, robustness will be guaranteed if the nominal loop function $l(s)$ lies above the related design bounds and does not enter the U-Contours. Also, it must not intersect the critical point (-180°, 0 dB).

Fig. 7*b* demonstrates a possible controller with the parameters of $K = -18$, $T_1 = 8.4$ and $T_2 = 33$, satisfying the QFT bounds.

7.2 Design of FD filters $Q_i(s)$, $i = 1, 2$

7.2.1 Design of $Q_1(s)$ to detect the actuator fault:

The residual reference model for the detection of actuator faults is computed using Theorem 1, with the following matrices for the selected nominal plant

$$\mathbf{B}_\mathrm{d} = \mathbf{B}, \quad \mathbf{B}_\mathrm{f} = \mathbf{B}, \quad \mathbf{D}_\mathrm{f} = 0, \quad \mathbf{D}_\mathrm{d} = 1 \tag{22}$$

To investigate the effect of the actuator fault on the frequency response, $\mathbf{D}_\mathrm{f}$ is assumed to be zero. In addition, $\mathbf{D}_\mathrm{d}$ has been set to unity so as to measure the actual effect of noise on the output measurement. The obtained residual reference model is then given by

$$M_1(s) = \frac{-47.89s}{(s^2+20.55s+128.4)(s^2+0.2802s+50.43)} \tag{23}$$

Since both disturbance rejection and FD cannot be simultaneously achieved in a similar range of frequency and the effect of ΔV_ref has been minimised over $\omega = [2.5, 12.5]$(rad/s), the range of FD is selected $\tilde{\omega} \in [0.1, 1] \cup [15, 20]$(rad/s) so as to consider both transient and steady-state behaviours. This fact that $|M_1(j\omega)|$ is nearly zero over $\tilde{\omega}$ arises from the magnitude frequency response of the SIMB which is almost zero over this frequency range. Such a residual reference model does not result in a desirable actuator FD characteristic if there is significant noise on the output measurement. In such cases, the use of dynamical weight matrices (function) is an alternative approach by which the obtained residual reference model (23) can be further modified and improved. Therefore the residual model reference (23) is multiplied by the weighting TF $W_{f_1}(s)$, in order to amplify the gain of the residual reference model over the frequency range in which FD is feasible

$$W_{f_1}(s) = -\frac{100((s/1)^2+s/1+1)((s/10)^2+s/10+1)}{((s/0.1)^2+s/0.1+1)((s/20)^2+s/20+1)} \tag{24}$$

The final residual reference model is, thus, taken to be

$$M_1(s) = \frac{1.9s(s^2+s+1)(s^2+10s+100)}{(s^2+0.1s+0.01)(s^2+0.2802s+50.43)(s^2+20.55s+128.4)(s^2+20s+400)} \tag{25}$$

Fig. 8 shows bode magnitude plots of (23) and modified residual reference model (25) as well as the range of frequencies which are dedicated for disturbance decoupling and actuator FD.

doi: 10.1049/iet-cta:20070382

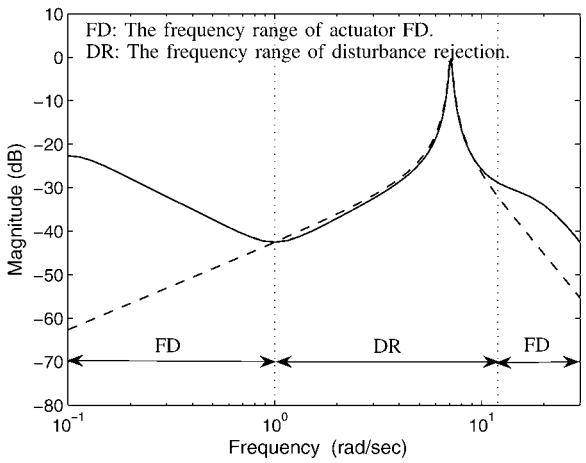

Figure 8 *'Dashed' denotes the residual reference $M_1(s)$ obtained through Theorem 1, and 'solid' denotes the modified residual reference $M_1(s)$ to amplify the effect of actuator fault over the FD design frequencies*

An error magnitude of 0.1 between the actual and reference residual models can be allowed by setting

$$E_{d_1}(s) = 0.1 \tag{26}$$

Fig. 9*a* shows the obtained design bounds for the actuator FD filter through Theorem 2. As is usual in practice, a low pass filter is added to the FD structure to mitigate the effect of high-frequency noise. A trial and error approach can be adopted to tune the actuator FD filter of (27). The design satisfies the performance constraints while also exhibiting very worthwhile low-order and low-bandwidth characteristics

$$Q_1(s) = \frac{10}{(s+0.1)} \tag{27}$$

7.2.2 Design of $Q_2(s)$ to detect the sensor fault:

The design procedure is now repeated using the approach motivated by Theorem 2. The residual reference model for the detection of sensor faults is computed using Theorem 1, incorporating the following matrices for the nominal plant

$$\begin{aligned} \mathbf{B}_{\mathrm{d}} &= \mathbf{B}, \quad \mathbf{B}_{\mathrm{f}} = [0 \quad 0 \quad 0 \quad 0]^{\mathrm{T}} \\ \mathbf{D}_{\mathrm{f}} &= 1, \quad \mathbf{D}_{\mathrm{d}} = 1 \end{aligned} \tag{28}$$

To investigate the effect of the sensor fault in this paradigm, $\mathbf{B}_{\mathrm{f}}$ has been assumed to be the zero vector. In addition, $\mathbf{D}_{\mathrm{d}}$ has been set to unity to consider the effect of noise on the output measurement. Equation (29) gives the TF of the obtained residual reference

$$M_2(s) = \frac{(s^2+20.41s+123.7)(s^2+0.4183s+52.35)}{(s^2+20.55s+128.4)(s^2+0.2802s+50.43)} \tag{29}$$

An appropriate engineering interpretation for the resulting $M_2(s)$ is that, in DC gain terms, the magnitude of the residual signal should closely track the actual signal produced by a sensor fault when it occurs. The desired FD error $E_{d_2}(s)$ is set to (30) to guarantee a zero steady-state error between reference and actual residual models

$$E_{d_2}(s) = \frac{0.25s}{(s+0.5)(s+5)} \tag{30}$$

A frequency range of $\tilde{\omega} = \{0.2, 0.5, 1, 5\}$(rad/s) is selected to generate the filter design bounds. Fig. 9*b* illustrates the

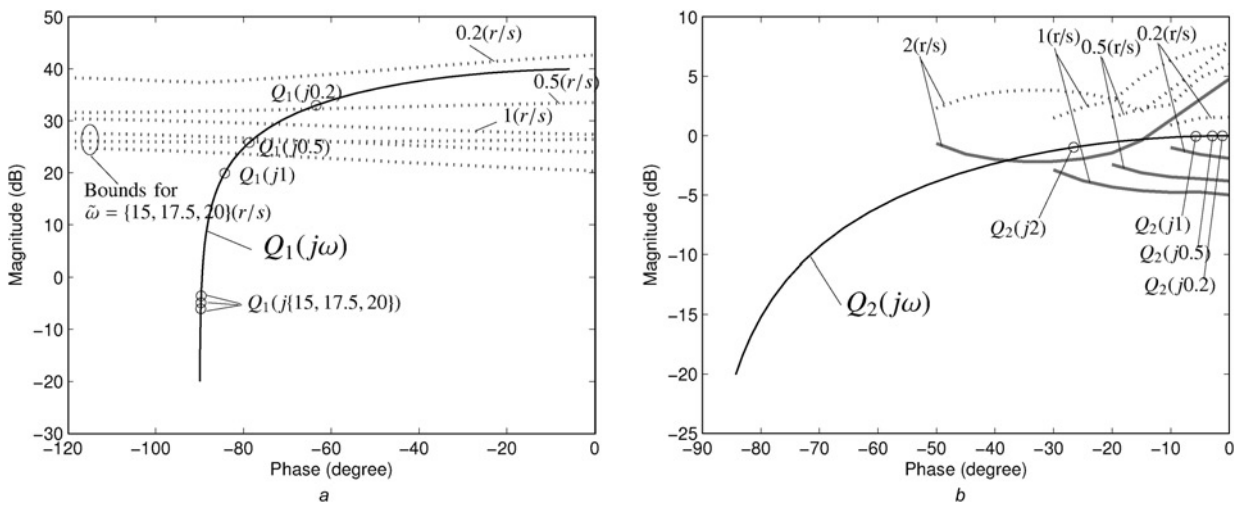

Figure 9 *Illustration of design bounds for shaping $Q_1(s)$ and $M_2(s)$*

The FD filters must lie above 'solid' line and below 'dot' line at each frequency
$(r/s) \triangleq$ (rad/s)
a Design of actuator FD filter $Q_1(s)$
b Design of sensor FD filter $Q_2(s)$

doi: 10.1049/iet-cta:20070382

constraints and the frequency response of a low-bandwidth filter that satisfies the performance constraint bounds. It is characterised by an intuitively appealing low-order TF

$$Q_2(s) = \frac{10}{(s+10)} \tag{31}$$

7.3 Threshold values and performance analysis

The effectiveness of the proposed QFT-based FDI approach in the presence of sensor fault has been investigated in [17]. In this paper, a more complicated scenario is presented. Both the actuator and sensor faults, $f_1(t)$ and $f_2(t)$, are applied as overlapped pulses occurring from $t = 20$ s until $t = 40$ s and from $t = 30$ s to $t = 50$ s, respectively. The disturbance $\Delta V_{\text{ref}}(t)$ is modelled as a number of randomly selected sinusoidal signals with different phases within the frequency range of $\omega = \{2.5, 12.5\}$(rad/s), added together and biased for 0.05 pu from $t = 5$ s until $t = 100$ s. Fig. 10 shows the considered disturbance, and actuator and sensor fault to the system. A band-limited white noise with a power of 10^{-6} (zero-order hold with sampling time 0.1 s) is also considered on the measured signal $y_m(t)$. Throughout the simulations, the detection window has been selected as $\tau = 50$ s. Table 1 shows a representative selection of sample plants over the plant uncertainty region.

The actuator and sensor residuals corresponding to the selected plants of Table 1 are shown in Figs. 11*a* and 11*b*, respectively. They confirm that: (1) the negative effects of ΔV_{ref} have satisfactorily been reduced and (2) the generated residuals react satisfactorily to the faults as soon as they occur.

Remark 4: As mentioned in Section 1, there is an unavoidable interaction between actuator and sensor fault residuals and therefore between their evaluation signals.

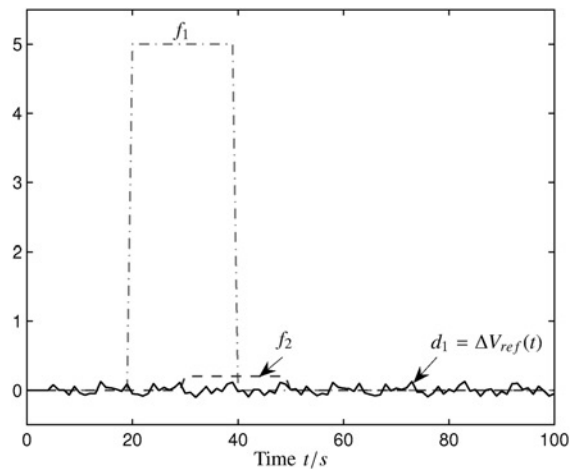

Figure 10 *Disturbance, $d_1(t) = \Delta V_{ref}$, actuator and sensor faults, $f_1(t)$ and $f_2(t)$, applied to the system*

Table 1 Three plant cases over the uncertainty region, [29]

	P_m, pu	Q_m, pu	X_e, pu
case1	0.8	0.4	0.2
case2	0.8	0.0	0.6
case3	1.0	0.5	0.7

The selection of FDI threshold values in order to appropriately distinguish between the (occurrence time of) actuator and sensor faults would be one of the significant challenges. In the following, it is explained how the aforementioned issue is addressed for this case study. No new point of principle arises in an intuitive extension of the methodology to different applications.

Figs. 12*a* and 12*b* illustrate the evaluation signals corresponding to the obtained residuals. Fig. 12*a* shows that after the appearance of the actuator fault at $t = 20$ s, the corresponding evaluation signal will increase in the detection window time. Note in Fig. 11 how the effect of a sensor fault will appear in a corresponding actuator-fault residual and evaluation signal. The effect of the actuator fault on the sensor fault in this case is negligable because the plant is low-gain. By defining an upper bound for the threshold value of the actuator-fault evaluation signal, the (occurrence time of) actuator and sensor faults are easily distinguished as shown in Fig. 12*a*. In practice, saturation constraints should be taken into account when selecting threshold values. By considering the fault-free system, $\|r_{d_1}(t)\|_2$, the following decision algorithm is given. There is no actuator fault if $\|\tilde{r}_1(t)\|_2 < 0.05$. If $\|\tilde{r}_1(t)\|_2 > 0.05\, AND\, \|\tilde{r}_1(t)\|_2 < 0.2$ then the actuator fault has occurred and if $\|\tilde{r}_1(t)\|_2 > 0.2$ then the sensor fault has occurred. Subsequently, by selecting sensor FDI threshold value according to $J_{\text{th}_2} = 0.01$, occurrence of the sensor a faults is easily detectable from $\|\tilde{r}_2(t)\|$ and $\|r_{d_2}(t)\|$, as illustrated in Fig. 12*b*.

7.4 Benchmark comparative study

A comparison is made between the proposed methodology and two proven strategies, H_2/H_∞ [14] and H_∞/LMI [11].

7.4.1 The mixed H_2/H_∞ FD approach: In [14], the residual signal is given by

$$\begin{aligned} \dot{\mathbf{x}} &= (\mathbf{A} - \mathbf{KC})\mathbf{x} + [\mathbf{B} - \mathbf{KD} \quad \mathbf{K}][u \quad y_m]^{\mathrm{T}} \\ r &= -\mathbf{Cx} + [-\mathbf{D} \quad 1][u \quad y_m]^{\mathrm{T}} \end{aligned} \tag{32}$$

The FD design parameter $\mathbf{K}$ is obtained through the convex minimisation problem (18) in [14], which results in

$$\mathbf{K} = [0.0017 \quad 0.5430 \quad -0.7129 \quad -17.4635]^{\mathrm{T}} \tag{33}$$

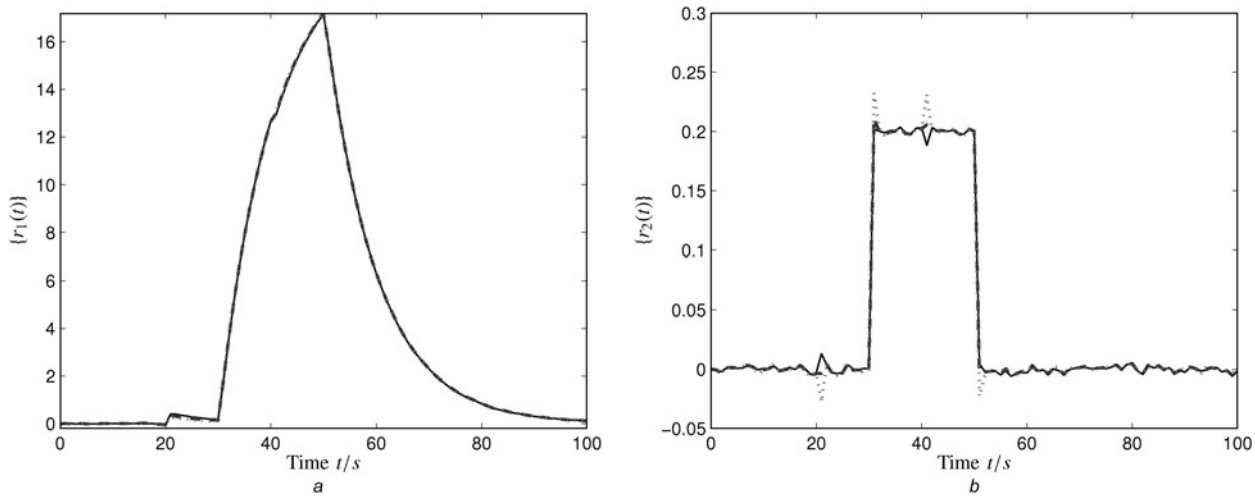

Figure 11 *Obtained residuals for the plant cases in Table 1*

This figure shows the robustness against exogenous disturbance and sensitivity to the faults
a Actuator-fault residuals
b Sensor-fault residuals

Fig. 13 shows the residual obtained by using (32) and (33). To be more clarified, the vertical axis is zoomed in as shown in Fig. 13*b*. Fig. 13*a* illustrates that the H_2/H_∞-based FD approach cannot guarantee residual stability over the whole uncertainty region even for detectable pair $(\mathbf{C}, \mathbf{A})$. Furthermore, simulation results show that the actuator fault is not detectable even for stable residuals as shown in Fig. 13*b*.

7.4.2 The mixed H_∞/LMI FDI approach: In [11], the proposed model-matching problem is solved by minimising the H_∞ norm of the difference between the residual reference model and the actual residual. In this technique, the residual is given by

$$\begin{aligned} \dot{\hat{\mathbf{x}}} &= (\mathbf{A} - \mathbf{HC})\hat{\mathbf{x}} + [\mathbf{B} - \mathbf{HD} \quad \mathbf{H}][u \quad y_m]^{\mathrm{T}} \\ \hat{y}_m &= \mathbf{C}\hat{\mathbf{x}} + \mathbf{D}u \\ r &= V(y_m - \hat{y}_m) \end{aligned} \tag{34}$$

where $\hat{\mathbf{x}}$ and $\hat{y}_m$ denote the estimated state vector and the system output, respectively. The FD design parameters $\mathbf{H}$ and V are obtained through the Theorem 2 in [11], which results in

$$\begin{aligned} \mathbf{H} &= [-15.9 \quad 3.5 \quad -4.2 \quad 100.88]^{\mathrm{T}}, \\ V &= -4.3105 \end{aligned} \tag{35}$$

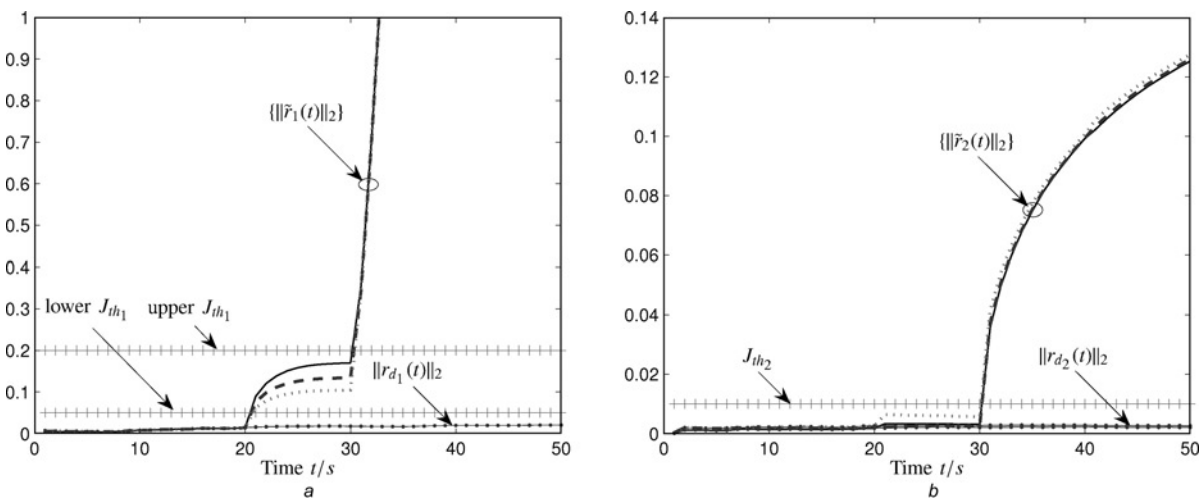

Figure 12 *Evaluation signals and corresponding FD threshold values, for the plant cases in Table 1*

a Evaluation of actuator-fault residuals
b Evaluation of sensor-fault residuals

doi: 10.1049/iet-cta:20070382

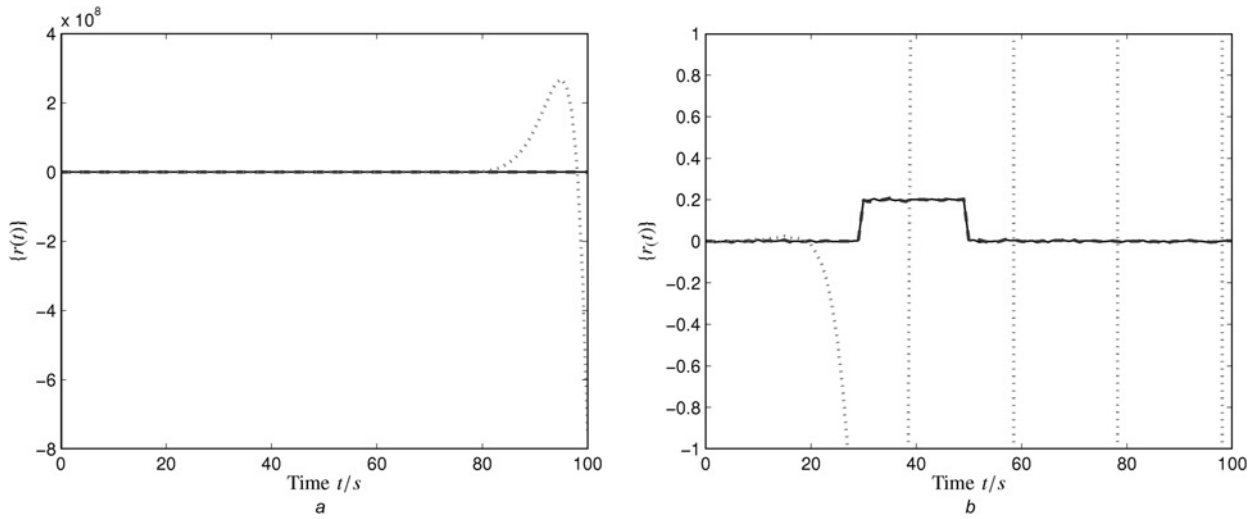

Figure 13 *The residual signals generated by the H_2/H_∞ FD technique [14] for the plant cases in Table 1*

The residual is unstable for the plant case 3
a Unzoomed residual
b Zoomed residual

It is simple to show that by choosing

$$\mathbf{E}_1 = [0\ \ -0.1\ \ 0.2\ \ -0.3]^{\mathrm{T}}, \quad \mathbf{E}_2 = [0\ \ 0\ \ 0\ \ -1.5]^{\mathrm{T}},$$
$$\mathbf{F}_2 = 0.1, \mathbf{F}_1 = 0.1\ \mathbf{I}_{4\times 4}$$

the uncertainty region of the state-space representation (6) would be the same as the proposed parametric uncertainty model (20) over the range of P_m: 0.4 to 1.0(pu), Q_m: -0.2 to 0.5(pu), and X_e: 0.0 to 0.7(pu).

In contrast to H_2/H_∞, Fig. 14 shows that the H_∞/LMI-based FDI approach results in stable residuals over the uncertainty region, however, similar to the mixed H_2/H_∞ technique [14], the actuator fault is still not detectable from the obtained residual. Moreover, the QFT-based FDI system results in a first-order FD filter which is much easier to implement than the fourth-order FD filters that are obtained through the H_2/H_∞ and H_∞/LMI techniques.

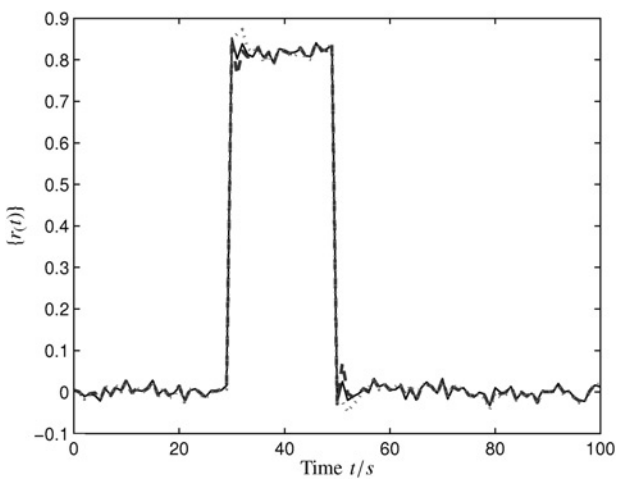

Figure 14 *Residual signals generated by the H_∞/LMI FDI technique [11], for the plant cases in Table 1*

Remark 5

a. Based on the proposed simulation results, it can be concluded that the FD techniques H_2/H_∞ and H_∞/LMI will fail to detect the fault associated with low-gain residual reference model.

b. Consider the scenario where the fault associated with the low-gain residual reference model happens after, but during the same detection window as, a fault associated with a much higher-gain residual reference model. It should be noted how in this scenario, the QFT approach exhibits a jump on the residual at the time that the second fault (i.e. the fault with the lower-gain residual reference model) occurs. However, the selection of threshold values will be rather complicated here because of the cross-coupling effects that exist. In the general case, the model-based isolation technique for such a scenario is an open and challenging issue.

8 Conclusion

A novel design methodology that generates robust residual signals for SISO systems has been presented in this work. A two-degree-of-freedom design framework based on shaping of the frequency response has been introduced to optimally design an integrated control and detection filter that is simultaneously robust to uncertainties as well as disturbances. As the proposed technique explicitly captures exact phase information, it is an effective design tool for both minimum and non-minimum phase plants. A SMIB power system has been employed to demonstrate the

doi: 10.1049/iet-cta:20070382

effectiveness of the proposed approach. Simulation results have shown that a satisfactory level of performance can be achieved where both actuator and sensor faults have occurred during the same time window.

9 Acknowledgments

This work was supported by Science Foundation Ireland under grant No. 05RFAPCMS0048. This work was partially supported by the Centre for Embedded Software Systems, during the visit of the first author from Aalborg University, Denmark. The authors gratefully acknowledge the contribution of Prof. Jakob Stoustrup to this work by the many fruitful discussions that he had participated in and the helpful advice that he had provided throughout the work. Special thanks are extended to the editor and anonymous reviewers for many fruitful comments that helped improve the quality of the work.

10 References

[1] BLANKE M., KINNAERT M., LUNZE J., STAROSWIECKI M.: 'Diagnosis and fault-tolerant control' (Springer, 2006, 2nd edn.)

[2] BLANKE M., IZADI-ZAMANABADI R., BOGH S.A., LUNAU C.P.: 'Fault tolerant control - a holistic view', *Control Eng. Prac.*, 1997, **5**, pp. 693–702

[3] CHEN J., PATTON R.J.: 'Robust model-based fault diagnosis for dynamic systems' (Kluwer Academic Publishers, 1999)

[4] GERTLER J.J.: 'Fault detection and diagnosis in engineering systems' (Marcel Dekker, Inc., 1998)

[5] FRANK P.M.: 'Enhancement of robustness in observer-based fault detection', *Int. J. Control*, 1994, **59**, (4), pp. 955–981

[6] FRANK P.M., DING X.: 'Survey of robust residual generation and evaluation methods in observer-based fault detection systems', *J. Process Control*, 1997, **7**, (6), pp. 403–424

[7] ISERMANN R.: 'Process fault detection based on modelling and estimation methods', *Automatica*, 1984, **20**, pp. 387–404

[8] KALLESOE C.S., COCQUEMPOT V., IZADI-ZAMANABADI R.: 'Model based fault detection in a centrifugal pump application', *IEEE Trans. Control Syst. Techn.*, 2006, **14**, (2), pp. 204–215

[9] STOUSTRUP J., GRIMBLE M., NIEMANN H.: 'Design of integrated systems for the control and detection of actuator/sensor faults', *Sensor Rev.*, 1997, **17**, (2), pp. 138–149

[10] RANK M., NIEMANN H.: 'Norm based design of fault detectors', *Int. J. Control*, 1999, **72**, (9), pp. 773–783

[11] ZHONG M., DING S.X., LAM J., WANG H.: 'An LMI approach to design robust fault detection filter for uncertain LTI systems', *Automatica*, 2003, **39**, pp. 543–550

[12] KHOSROWJERDI M.J., NIKOUKHAH R., SAFARI-SHAD N.: 'A mixed H_2/H_∞ approach to simultaneous fault detection and control', *Automatica*, 2004, **40**, (2), pp. 261–267

[13] HENRY D., ZOLGHADRI A.: 'Design and analysis of robust residual generators for systems under feedback control', *Automatica*, 2005, **41**, pp. 251–264

[14] KHOSROWJERDI M.J., NIKOUKHAH R., SAFARI-SHAD N.: 'Fault detection in a mixed H_2/H_∞ setting', *IEEE Trans. Autom. Control*, 2005, **50**, (7), pp. 1063–1068

[15] KARPENKO M., SEPEHRI N.: 'Fault-tolerant control of a servohydraulic positioning system with crossport leakage', *IEEE Trans. Control Syst. Technol.*, 2005, **13**, (1), pp. 155–161

[16] EMAMI-NAEINI A., AKHTER M.M., ROCK S.M.: 'Effect of model uncertainty on failure detection: The threshold selector', *IEEE Trans. Autom. Control*, 1988, **33**, (12), pp. 1106–1115

[17] ALAVI S.M.M., IZADI-ZAMANABDI R., HAYES M.J.: 'On the generation of a robust residual for closed-loop control systems that exhibit sensor faults'. IET Proc. Irish Signals and Systems Conference N. Ireland, 2007, pp. 59–66

[18] DOYLE J., FRANCIS B., TANNENBAUM A.: 'Feedback control theory' (MacMillan Publishing Co., 1990)

[19] HOROWITZ I.: 'Survey of quantitative feedback theory (QFT)', *Int. J. Robust Nonlinear Control*, 2001, **11**, pp. 887–921

[20] HOROWITZ I., SIDI M.: 'Synthesis of feedback systems with large plant ignorance for prescribed time-domain tolerances', *Int. J. Control*, 1972, **16**, pp. 287–309

[21] HOUPIS C.H., RASMUSSEN S.J., GARCIA-SANZ M.: 'Quantitative feedback theory fundamentals and applications' (Taylor & Francis, CRC Press, 2006, 2nd edn.)

[22] CHAIT Y., YANIV O.: 'Multi-input/single-output computer aided control design using the Quantitative Feedback Theory', *Int. J. Robust Nonlinear Control*, 1993, **3**, pp. 47–54

[23] FRISK E., NIELSEN L.: 'Robust residual generation for diagnosis including a reference model for residual behavior', *Automatica*, 2006, **42**, pp. 437–445

[24] DING S.X., DING E.L., JEINSCH T.: 'A new optimization approach to the design of fault detection filters'. Proc. SAFEPROCESS'2000, Hungary, 2000, pp. 250–255

[25] BOJE E.: 'Pre-filter design for tracking error specifications in QFT', *Int. J. Robust Nonlinear Control*, 2003, **13**, pp. 637–642

doi: 10.1049/iet-cta:20070382

[26] ALAVI S.M.M., KHAKI-SEDIGH A., LABIBI B., HAYES M.J.: 'Improved multivariable quantitative feedback design for tracking error specifications', *IET Control Theory Appl.*, 2007, **1**, (4), pp. 1046–1053

[27] HAYES M.J., ALAVI S.M.M., VAN DE VEN P.: 'An improved active queue management scheme using a two-degree-of-freedom feedback system'. Proc. European Control Conference, Greece, 2007, pp. 1873–1878

[28] ANDERSON P.M., FOUAD A.A.: 'Power system control and stability' (IEEE Press, Revised Printing, 1994)

[29] RAO P.S., SEN I.: 'Robust tuning of power system stabilizers using QFT', *IEEE Trans. Control Syst. Technol.*, 1999, **7**, (4), pp. 478–486

[30] BORGHESANI C., CHAIT Y., YANIV O.: 'The QFT frequency domain control design toolbox for use with MATLAB' (Terasoft, Inc, 2003)

11 Appendix 1: system dynamic equations

Suppose the active power, P_m, reactive power, Q_m, impedance of the transmission line, X_e and nominal terminal voltage, V_{t_0} are given. Then, K_1 to K_6 are computed by the following equations

$$V_d = P_m V_{t_0} / \sqrt{P_m^2 + (Q_m + V_{t_0}^2 / X_q)^2}$$

$$V_q = \sqrt{V_{t_0}^2 - V_d^2}$$

$$V_t = \sqrt{V_d^2 + V_q^2}$$

$$I_d = (P_m - I_q V_q)/V_d$$

$$I_q = V_d / X_q$$

$$e_q' = V_q + X_d' I_d$$

$$V_{od} = V_d + X_e I_q$$

$$V_{oq} = V_q - X_e I_d$$

$$E_{\mathrm{b}} = \sqrt{V_{od}^2 + V_{oq}^2}$$

$$\delta_0 = \tan^{-1}(V_{od}/V_{oq})$$

$$\begin{bmatrix} K_1 \\ K_2 \end{bmatrix} = \begin{bmatrix} 0 \\ I_q \end{bmatrix} + \begin{bmatrix} \dfrac{E_{\mathrm{b}} \sin \delta_0}{X_e + X_d'} & \dfrac{E_{\mathrm{b}} \cos \delta_0}{X_e + X_q} \\ \dfrac{1}{X_e + X_d'} & 0 \end{bmatrix} \times \begin{bmatrix} (X_q - X_d') I_q \\ e_q' + (X_q - X_d') I_d \end{bmatrix}$$

$$\begin{bmatrix} K_3 \\ K_4 \end{bmatrix} = \begin{bmatrix} \dfrac{X_e + X_d'}{X_e + X_d} \\ \dfrac{X_d - X_d'}{X_e + X_d'} E_{\mathrm{b}} \sin \delta_0 \end{bmatrix}$$

$$\begin{bmatrix} K_5 \\ K_6 \end{bmatrix} = \begin{bmatrix} 0 \\ V_q / V_t \end{bmatrix} + \begin{bmatrix} \dfrac{E_{\mathrm{b}} \sin \delta_0}{X_e + X_d'} & \dfrac{E_{\mathrm{b}} \cos \delta_0}{X_e + X_q} \\ \dfrac{1}{X_e + X_d'} & 0 \end{bmatrix} \begin{bmatrix} -X_d' V_q / V_t \\ X_q V_d / V_t \end{bmatrix}$$

where subscript 0 is steady state value, Δ the small deviation, δ the rotor angle, ϖ the rotor angular speed, e_q' the voltage proportional to field flux linkage, E_{fd} the field voltage, ω_{B} the base speed, V_{ref} the AVR reference input, K_{A} the AVR gain, T_{A} the AVR time constant, H the rotor inertia constant, V_{t} the generator terminal voltage, T_{do}' the d-axis transient open circuit time, X_d' the d-axis transient reactance, X_d, X_q the d- and q-axes synchronous reactances, I_d, I_q the d- and q-axes generator currents, V_d, V_q the d- and q-axes generator voltages, E_{b} the infinite bus voltage, T_m the mechanical torque.

12 Appendix 2: system data

The system data is given by: $X_d = 2.0$ pu, $X_d' = 0.244$ pu, $X_q = 1.91$ pu, $T_{do}' = 4.18$ sec, $E_{\mathrm{b}} = 1.0$ pu, $H = 3.25$ sec, $\omega_{\mathrm{B}} = 314.15$ rad/sec, $K_{\mathrm{A}} = 50.0$ and $T_{\mathrm{A}} = 0.05$ sec.

doi: 10.1049/iet-cta:20070382